Segmentation of Pulmonary Fissures on Diagnostic CT – Preliminary Experience*

Jingbin Wang, MEng,[a] Margrit Betke, PhD,[a] and Jane P. Ko, MD[b]

[a] Computer Science Department, Boston University, Boston, MA, USA
[b] Department of Radiology, New York University, New York, NY, USA

ABSTRACT

We describe a new approach to detect the fissures between the lobes of the lungs in computed tomography (CT) scans. We focus on the detection of the major fissures in diagnostic CT. Our approach is to first find a region containing the fissure and then extract the fissure within this region by analyzing local features. We developed a "marching-bar method" to segment the region containing the fissure. After this region is computed for an initial slice, fissure extraction in consecutive slices is performed using the location information inherited from previous slices.

1. Introduction

With the emergence of new digital imaging technologies, large data sets of images are being created that are often difficult to analyze accurately and efficiently by hand. Computer-aided diagnosis (CAD) systems have therefore been developed to automate the analysis of chest computed tomography (CT) scans and support the diagnosis of numerous diseases, for example, lung cancer or emphysema [2, 1, 4]. To become a reliable clinical tool, a chest CAD system must be able to segment and model the lungs and its structures accurately. The work presented here contributes to the current efforts in designing reliable segmentation methods for chest CT. In particular, we describe a new method for extracting pulmonary fissures.

A pulmonary fissure is a boundary between two lung lobes which are distinct parts of the lung. Identifying the fissures on CT images is crucial for understanding the anatomy of the imaged lung. A large structure adjacent to a fissure, for example, could indicate the occurrence of a nodule, since normal lung structures generally do not appear within a few millimeters of a fissure.

Our focus is on developing a method that can be applied to diagnostic CT. Diagnostic CT has wide clinical use. Patients are generally imaged in 5 mm to 7 mm sections in which the contours of the fissures appear as extremely faint structures due to partial volume averaging. Although a fissure is geometrically a surface, we follow common practice and use the term "fissure" to also describe the fissure cross-section in an image.

*Financial support by the Whitaker Foundation, National Science Foundation, Office of Naval Research, and National Institutes of Health is gratefully acknowledged.

The left lung has two lobes separated by a major fissure, and the right lung has three lobes separated by a minor and a major fissure. On a diagnostic CT image, the major fissure can be seen as a faint curve spanning from the medial to the lateral border of the lung. When a CT scan is viewed in the axial plane from the upper thorax down to the lower thorax, the major fissures appear to move from the posterior to the anterior in both lungs. The minor fissure in the right lung is oriented in the axial plane and can be best viewed in the sagittal plane. We focus here on the detection of the major fissures.

Few papers in the literature have discussed the topic of fissure segmentation. They focus on thin-section CT, where fissures appear as avascular lines. A method by Kubo et al. [5] detects fissures in 1 mm CT sections by converting the original CT image into a binary image with a fixed threshold of -300 Hounsfield Units (HU) and then analyzing the binary image with morphological operations. Zhang and Reinhardt [6] work with 3 mm CT sections and use a fuzzy set approach that is also threshold based.

To develop a fissure segmentation method for diagnostic CT, we must address two main problems: (1) It is difficult to designate a favorable fixed threshold due to the wide range of possible densities of non-fissure structures within the lung. (2) The density values of a fissure are so low that it often seems imperceptible. As a result, the magnitude of the density gradients in the region around the fissure, the "fissure region of interest" (ROI), is generally very small. Due to these problems, traditional threshold-based methods are of limited use.

We developed a "marching-bar method" to segment the fissure ROI, which we then analyze to extract the fissure. Once the fissure is computed in an initial slice, the fissures are extracted in consecutive slices using location information inherited from the fissure ROI in previous slices. Our goal is to develop three-dimensional models of the lobes of both lungs. With a future system that can reliably segment the lung lobes, we hope to support a radiologist in the evaluation of chest CT scans.

2. Method

The framework of our two-step algorithm is shown in Fig. 1. In the initial step, an automatic thresholding method is used to produce a binary image of the lung parenchyma, which was segmented by a previously described method [4]. We developed a "marching-bar method" to mark the fissure ROI by sweeping a "bar" to the lateral and medial borders of the lungs. In this process, the length of the bar can adaptively change at each step, so that the vertically longest local region that does not contain large gradient changes is covered by the bar. From the given fissure ROI, the fissure is then segmented.

2.1. Detection of the Fissure Region

The fissure ROI is detected in two phases – a thresholding phase and a marching-bar phase. In the thresholding phase, the grayscale values of the pixels in the segmented lungs are automatically converted into binary values. The resulting binary image

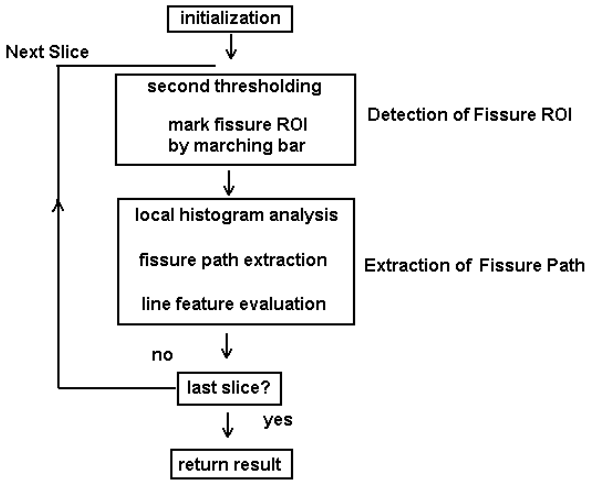

Figure 1. System overview.

contains white pixels for lung structures, such as bronchi, vessels, and nodules, and black pixels for the fissures and the aerated lung. The marching-bar phase of our algorithm is then applied to the binary image of the lungs.

The thresholding method applied is known as the P-tile method [3]. The value P is the desired ratio of the number of white pixels to the number of black pixels. In our current implementation, we set $P = 25\%$ after extensive experimentation. To automatically determine the threshold that produces four times as many black pixels as white pixels, the histogram of the grayscale values of the pixels in the lungs is evaluated.

We define a "bar" to be a vertical line segment of variable length. In our current implementation, its length can range from 4 mm to 20 mm. In order to find the fissure ROI in the first slice, the start point for creating the first marching bar needs to be designated manually. In most cases, this point may be anywhere inside the fissure ROI. Then the first marching bar is created by growing it from the start point in both vertical directions, namely, upwards and downwards. If either end of the bar hits a white pixel, the bar stops extending in that direction. The current bar also stops extending if its maximal length is reached.

Once a fully grown bar is obtained, the horizontally adjacent pixels of its midpoint are used as the respective start points for new bars on the left and right sides. The bars are grown by the same process as described above. In this manner, a bar "marches" horizontally towards the lateral lung border and another bar towards the medial border (see Fig. 2). The "march" stops when either end of the current bar hits the lung border. The pixels that are covered by the marching bar compose a connected "dark" region, the fissure ROI. The fissure ROI, therefor, can be seen as a set of side-by-side bars.

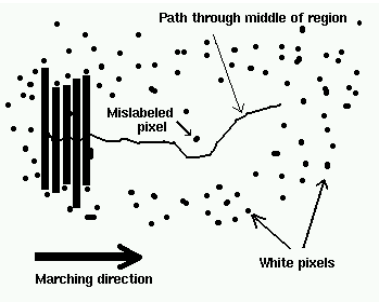

Figure 2. The marching-bar method.

Only the initial CT slice needs manual intervention to determine the start point of the first bar. In subsequent slices, the start point can be determined automatically by using the fissure ROI location in the previous slice.

2.2. Fissure Detection within Fissure Region

Once the fissure ROI is computed for some slice, additional local feature analysis is performed to determine the location of the fissure inside the region. Our general approach is to extract a path through the fissure ROI. We call this path the "fissure path." A straightforward approach would be to connect the midpoints of the bars and create a curve as shown in Fig. 2. However, there may be a few pixels on the fissure that were labeled "white," as illustrated in Fig. 2. We therefore go back to the original CT image and re-process the grayscale values in the fissure region.

The P-tile method described in Section 2.1 is applied with $P = 0.5$ to obtain a new threshold $T.'$ All pixels in the fissure ROI with a grayscale value within the small range of the four gray levels $T', \ldots, T' + 3$ are initially considered to belong to the fissure. We call them "valid pixels."

Using the marching bar result, the following process is then performed to extract the complete fissure path. An arbitrary bar from the fissure ROI is selected as the starting bar and its valid pixels are detected. The valid pixels may comprise several continuous vertical segments. The tallest segment is marked as a piece of the fissure path, and its comprising pixels are added into the set of pixels F that define the fissure path. The endpoints of the segment define an initial estimate (H_{bottom}, H_{top}) of the vertical extent of the fissure path.

The process of computing vertical pixel segments is performed for the bars on the left and right side of initial bar. Among the detected segments, the tallest segment that overlaps with the computed vertical range of the fissure path is recorded as a new piece of the fissure path, and set F and endpoints (H_{bottom}, H_{top}) are updated. Threshold T' is also updated by averaging the grayscale values of all pixels in set F. The process is repeated for neighboring bars. In this manner, F is expanded until it finally represents the complete fissure path.

Some bars may not contain any segments that overlap with the vertical path range defined by (H_{bottom}, H_{top}). Such bars are skipped during the creation of the

fissure path. This may result in a discontinuous fissure path that is then reconnected by interpolation. In addition, a given starting bar may not contain any valid pixels or its valid pixels may not belong to the fissure. Therefore several starting bars are considered and their resulting fissure paths are candidate solutions which are evaluated further.

In order to decide among several candidate fissure paths, the curvature of the each path is evaluated at sample points along the path. In the current implementation, the longest path that most closely resembles a line is chosen as the final estimate for the fissure.

3. Results and Discussion

We tested a CT scan with a resolution of 512×512 pixels per slice and a slice thickness of 10 mm with a change in slice thickness to 5 mm through the hila. Some of our test images and results are shown in Fig. 3. The average root of the mean squared (RMS) error of the segmentation is 1.2 mm (see Fig. 4).

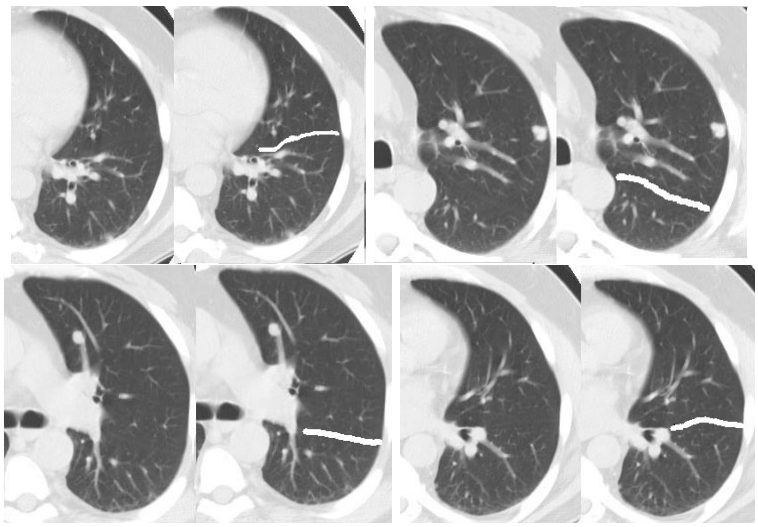

Figure 3. Examples of test images. The segmented fissures are shown as white curves.

Due to the anatomy and image characteristics of pulmonary fissures, it is generally a difficult problem to segment fissures from CT images. We use a two-step strategy – first segmenting a region containing the fissure and then finding the fissure within this region. We proposed this two-step approach, because we believe that it is much easier to perform feature analysis on a local region than on the whole lung.

By focusing on diagnostic CT, our goal was to develop an algorithm that works for low-resolution images and therefore has a strong potential to also work for higher-resolution images. We expect to be able to apply our marching-bar technique without extensive modifications to fissure detection on thin-section CT.

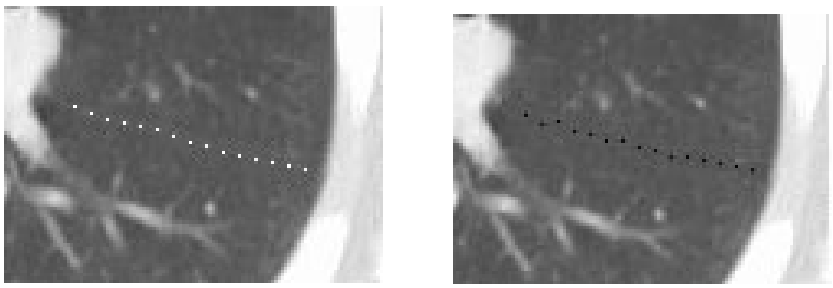

Figure 4. Validation. For each slice, the RMS error is computed for 15 points that are equally spaced on the hand-segmented (white points) and computed (black points) fissures.

The grayscale values of the fissures and the surrounding aerated lung are very similar, but the range of values may vary among scans, images, and even within an image. It is therefore difficult to ascertain a specific grayscale threshold to segment the fissure. The proposed method has the advantages that it determines thresholds based on local image regions and computes them automatically. In addition, the method is flexible in the sense that it can provide several ranked candidate solutions even if the fissure is barely detectable by the human eye.

Future work will include extensive testing of our methods. We are also planning to extend our methods and apply them to data sets that have abnormalities near or adjacent to the fissures.

REFERENCES

1. C. E. Brodley, A. Kak, J. Dy, C. R. Shyu, A. Aisen, and L. Broderick. Content-based retrieval from medical image databases: A synergy of human interaction, machine learning and computer vision. In *The Sixteenth National Conference on Artificial Intelligence*, pages 760–767, Orlando, FL, July 1999.
2. M. S. Brown, M. F. McNitt-Gray, J. G. Goldin, J. W. Suh, R. D. Sayre, and D. R. Aberle. Patient-specific models for lung nodule detection and surveillance in CT images. *IEEE Trans Med Imag*, 20(12):1205–1208, December 2001.
3. R. Jain, R. Kasturi, and B. Schunk. *Machine Vision*. McGraw Hill, 1995.
4. J. P. Ko and M. Betke. Chest CT: Automated nodule detection and assessment of change over time – preliminary experience. *Radiology*, 218(1):267–273, 2001.
5. M. Kubo, Y. Kawata, N. Niki, K. Eguchi, H. Ohmatsu, R. Kakinuma, M. Kaneko, M. Kusumoto, N. Moriyama, K. Mori, and H. Nishiyama. Automatic extraction of pulmonary fissures from multidetector-row CT images. In *Proc. IEEE International Conf. on Image Processing (ICIP'01)*, pages 1091–1094, 2001.
6. L. Zhang and J. M. Reinhardt. Detection of lung lobar fissures using fuzzy logic. In C.-T. Chen and A. V. Clough, editors, *Medical Imaging 1999: Physiology and Function from Multidimensional Images, SPIE Proceedings Vol. 3660*, pages 188–198, San Diego, CA, February 1999.